L_0 is the probability that a normal cell will be discarded on arrival in an arbitrary time slot and L_1 is the equivalent probability for a tagged cell. It can be shown that

$$L_0 = \frac{1}{\bar{a}_0}\sum_{n=0}^{B} S_n \left\{ \sum_{j=B-f(n)=1}^{\infty} [(j-B+f(n))a_{0,j}] \right\} \quad (4)$$

$$L_1 = \frac{1}{\bar{a}_1}\sum_{n=0}^{T}\left\{ S_n \left[\sum_{j=0}^{T-f(n)} \left[a_{0,j} \sum_{i=T-f(n)-j+1}^{\infty} [(i-T+f(n)+j)a_{1,i}] \right] + \bar{a}_1 \sum_{j=T-f(n)+1}^{\infty} a_{0,j} \right]\right\} + \sum_{n=T+1}^{B} S_n \quad (5)$$

where $\bar{a}_0 = \Sigma_1^\infty(ka_{0,k})$ is the mean bulk size (and also the mean arrival rate) for normal cells and $\bar{a}_1 = \Sigma_1^\infty(ka_{1,k})$ is the equivalent for tagged cells.

Numerical results: Some numerical results are obtained by assuming that the bulk size distributions of normal and tagged cells follow the following truncated Poisson processes:

$$a_{i,k} = \frac{\lambda_i^k e^{-\lambda_i}/k!}{\sum_{j=0}^{M} \lambda_i^j e^{-\lambda_i}/j!} = \frac{\lambda_i^k/k!}{\sum_{j=0}^{M} \frac{\lambda_i^j}{j!}} \quad \text{for } 0 \le k \le M \quad (6)$$

where $i = 0$ is for normal cells and $i = 1$ is for tagged cells.

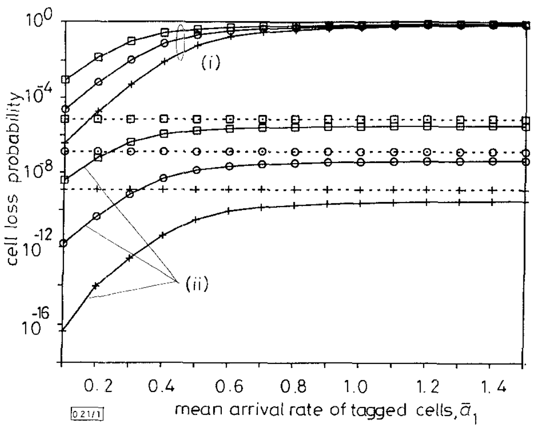

Fig. 1 *Cell loss probabilities of tagged and normal cells for B = 32 and T = 16*

(i) tagged cells
(ii) normal cells
+ $\bar{a}_0 = 0.5$
○ $\bar{a}_0 = 0.6$
□ $\bar{a}_0 = 0.7$

The results shown in Figs. 1 and 2 are obtained with $B = 32$, $M = 100$ and $\bar{a}_0 = 0.5$, 0.6 and 0.7. The difference between the two figures is that T is 16 in Fig. 1 and 20 in Fig. 2. Note that the cell loss probability for normal cells starts to level off at about $\bar{a} = 0.5$ for $\bar{a}_0 = 0.5$, $\bar{a}_1 = 0.4$ for $\bar{a}_0 = 0.6$ and $\bar{a}_1 = 0.3$ for $\bar{a}_0 = 0.7$. It appears that if $\bar{a}_0$ and other parameters are fixed while $\bar{a}$ is allowed to increase gradually, the cell loss probability for normal cells will start to level off at about $\bar{a}_1 = 1-\bar{a}_0$. In hindsight, this phenomenon can be explained by regarding the buffer as consisting of two parts: the first part consists of space for T cells which is shared by both the normal and tagged cells, and the second part consists of space for $B-T$ cells which is used exclusively by normal cells. When $\bar{a}_1$ increases beyond $1-\bar{a}_0$, the aggregate arrival rate exceeds unity; so, the shared portion becomes fully occupied at all times. Further increase in $\bar{a}_1$ will not result in a substantial increase in the loss probability of normal cells because, regardless of the traffic intensity of tagged cells, normal cells have the exclusive right to use the $B-T$ buffering spaces. This argument implies that the loss probability of normal cells at a partially shared buffer of size B and threshold T cannot be worse than if they are queued in a dedicated buffer of size $B-T$. The cell loss probabilities for normal cells in such a buffer for $\bar{a}_0 = 0.5$, 0.6 and 0.7 are shown as three horizontal dotted lines in Figs. 1 and 2. It can be seen that as $\bar{a}_1$ increases, the loss probabilities for normal cells move closer to the respective bounds, but never go beyond them.

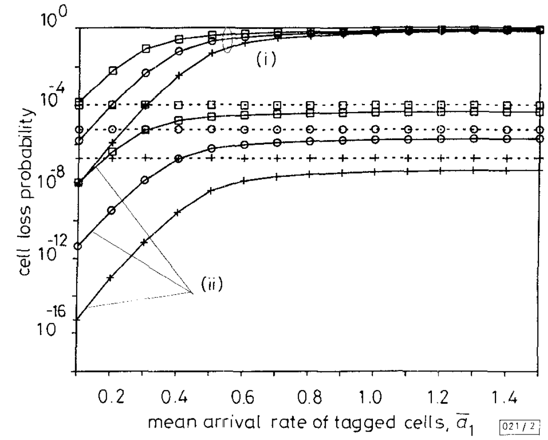

Fig. 2 *Cell loss probabilities of tagged and normal cells for B = 32 and T = 20*

(i) tagged cells
(ii) normal cells
+ $\bar{a}_0 = 0.5$
○ $\bar{a}_0 = 0.6$
□ $\bar{a}_0 = 0.7$

Conclusions: We have analysed the cell loss performance of normal and tagged cells at a threshold-based partially shared buffer. The results show that the cell loss requirement of normal cells can be met by proper dimensioning of buffer space and setting of threshold regardless of the traffic intensity of tagged cells. Hence, we conclude that, if all ATM nodes adopt this type of buffering, tagged cells can be admitted into the network at will to take advantage of unused bandwidth without degrading the QoS offered to contract-abiding ATM connections.

12 April 1996
Electronics Letters Online No: 19960822

T.H. Cheng, J.F. Chen and M.T. Yap (*School of Electrical and Electronic Engineering, Nanyang Technological University, Singapore*)

References

1 Draft Revised ITU-T Recommendation 1.371, 'Traffic control and congestion control in B-ISDN'. ITU-T, December 1994

2 COOPER, C.A., and PARK, K.I.: 'Toward a broadband congestion control strategy', *IEEE Netw. Mag.*, 1990, **4**, (3), pp. 18–23

3 BAJA, K., CIDON, I., and SOHRABY, K.: 'Congestion control for high speed packet switched networks'. IEEE INFOCOM 1990, pp. 520–526

4 LIPSKY, L.: 'Queueing theory: A linear algebraic approach' (Macmillan, 1992)

Optimisation of switching levels for adaptive modulation in slow Rayleigh fading

J.M. Torrance and L. Hanzo

Indexing terms: Adaptive systems, Modulation

Multi-dimensional minimisation techniques are used to optimise, for specific applications, the upper bound bit error rate (BER) and bits per symbol (BPS) performances of adaptive modulation schemes over Rayleigh channels. This is achieved by modifying the switching criteria for selecting the appropriate modulation scheme.

Introduction: Adaptive modulation exploits the variation in bit error rate (BER) performance of various modulation schemes to mitigate the effects of narrowband multipath radio channels. A suitable modulation scheme is used, on a frame by frame basis, depending upon the prevailing channel conditions. An appropriate method of determining the channel conditions, when there is a sufficiently low normalised Doppler frequency, is to use time division duplex (TDD). In such a system, reciprocity and the correlation between adjacent up and down link slots, are exploited by the transmitter. Therefore, when synthesising a frame, the transmitter estimates the signal level that will be received at the other end of the link for that frame, and selects the most appropriate modulation scheme. This Letter describes how to determine which modulation scheme is most suitable once the received signal level has been estimated.

Upper bound BER performance of adaptive modulation: In [1] it was shown that the upper bound BER performance of an adaptive modulation scheme of the type described in [2] is given by

$$P_a(S/N) = B^{-1}\begin{bmatrix} & 1 & \cdot\int_{l_1}^{l_2} P_b(s/N)\cdot F(s,S) & ds \\ + & 2 & \cdot\int_{l_2}^{l_3} P_q(s/N)\cdot F(s,S) & ds \\ + & 4 & \cdot\int_{l_3}^{l_4} P_{16}(s/N)\cdot F(s,S) & ds \\ + & 6 & \cdot\int_{l_4}^{\infty} P_{64}(s/N)\cdot F(s,S) & ds \end{bmatrix} \quad (1)$$

where l_1, l_2, l_3 and l_4 are the thresholds between transmission of BPSK, QPSK, square 16 point and square 64 point QAM, respectively, and B is the mean number of BPS. The BER performances of BPSK, QPSK, square 16 and 64 point QAM in a Gaussian channel against the signal-to-noise ratio (SNR), s/N, are given by $P_b(s/N)$, $P_q(s/N)$, $P_{16}(s/N)$ and $P_{64}(s/N)$, respectively. The probability density function (PDF) of the fading channel is given by $F(s, S)$, where s and S are the instantaneous and average signal power, respectively. The value of B is given by

$$\begin{aligned} B = 1\cdot\int_{l_1}^{l_2} F(s,S)ds + 2\cdot\int_{l_2}^{l_3} F(s,S)ds \\ + 4\cdot\int_{l_3}^{l_4} F(s,S)ds + 6\cdot\int_{l_4}^{\infty} F(s,S)ds \end{aligned} \quad (2)$$

Optimisation of switching levels: Adaptive modulation schemes may select the appropriate modulation level for the transmitted frame on the basis of either the number of errors encountered in the received frame or the received signal strength [3]. The former is only possible in a system that includes some error detection. The method proposed in this Letter is for selecting the switching values of l_1, l_2, l_3 and l_4 for an adaptive scheme on the basis of the received signal strength, in order to select the appropriate modulation level for each frame. The BER and BPS upper bound performance of an adaptive modulation scheme may be quickly evaluated with reference to [1] for a range of average channel SNRs. The difference between this upper bound performance and the desired performance can be used as a cost function for given modulation switching levels of l_1, l_2, l_3 and l_4. Minimisation of this cost function may be achieved iteratively by varying the switching levels l_1, l_2, l_3 and l_4 using Powell's algorithm [4].

The BER and BPS performances were evaluated for average channel SNRs in the range from 0 to 50dB in 1dB intervals. The cost function was defined as

$$Total\ Cost = \sum_{i=0}^{50} BER\ Cost(i) + BPS\ Cost(i) \quad (3)$$

where

$$BER\ Cost(i) = \begin{cases} 10\left[\log_{10}\left(\frac{BER_m(i)}{BER_d(i)}\right)\right] & \text{if } BER_m(i) > BER_d(i) \\ 0 & \text{otherwise} \end{cases} \quad (4)$$

$$BPS\ Cost(i) = \begin{cases} BPS_d(i) - BPS_m(i) & \text{if } BPS_d(i) > BPS_m(i) \\ 0 & \text{otherwise} \end{cases} \quad (5)$$

and $BER_m(i)$, $BER_d(i)$, $BPS_m(i)$ and $BPS_d(i)$ are, respectively, the measured and desired BER and BPS at an average channel SNR of i. It can be seen from eqns.. 3 – 5 that the cost function can only be positive, and increases when either the BER or the BPS performance become inferior to their desired performance at an average channel SNR of i. The cost function cannot be negative, therefore at high average channel SNRs, where both the BER and the BPS outperform their repective desired performance targets, the combined performance will be sacrificed. The advantage of this approach is that it reduces the minimum average channel SNR above which both desired BER and BPS performance criteria is achieved. However, the performance does improve at higher average SNRs owing to the favourable prevailing channel conditions. Eqn. 4 uses the logarithm function to increase the significance of small BERs. A weighting factor of 10 is used to bias the optimisation towards achieving the desired BER performance in preference to the BPS performance.

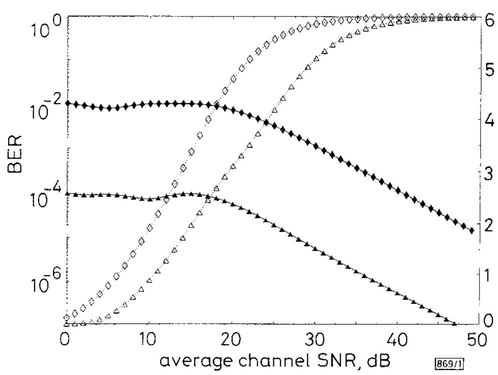

Fig. 1 *Upper bound BER and BPS performance of adaptive QAM in Rayleigh Channel optimised separately for speech (l_1 = 3.31, l_2 = 6.48, l_3 = 11.61 and l_4 = 17.64dB) and computer data (l_1 = 7.98, l_2 = 10.42, l_3 = 16.67 and l_4 = 26.33dB) transfer*

◆ speech optimised BER
◇ speech optimised BPS
▲ computer data optimised BER
△ computer data optimised BPS

Results and conclusion: Two desired system performance profiles were considered, one which was optimised for a speech codec with a target BER and BPS of 0.01 and, 4.5 respectively, and another intended for computer data transfer with target BER and BPS of 0.0001 and 3, respectively. The optimisation was performed for Rayleigh channel conditions and the initial condition for both minimisations was l_1 = 5 dB, l_2 = 8dB, l_3 = 14dB and l_4 = 20dB. After optimisation the values of l_1 = 3.31, l_2 = 6.48, l_3 = 11.61 and l_4 = 17.64 were registered for the speech system. For the computer data system the values of l_1 = 7.98, l_2 = 10.42, l_3 = 16.76 and l_4 = 26.33 were recorded. Considering Fig. 1, the desired BER is achieved between 0 and 50dBs for both the speech and computer data switching levels schemes. The targeted BPS performance is achieved at ~18 and 19dB average channel SNRs for the speech and computer data schemes, respectively. Observe in the figure that both the speech and data BER profiles outperform the BER requirements for average channel SNRs greater than these values. The system was capable of maintaining the target BER performances at extremely low average SNR values. This robust performance was achieved at the cost of reducing the BPS channel capacity below that of BPSK, which was possible owing to disabling transmissions for low instantaneous SNR values. To ensure that the optimisation for Rayleigh channel conditions did not yield switching values that were too specific, the same switching values were evaluated through Rician channels with K factors of 4 and 16. The performance through Rician channels was quite similar to that for Rayleigh channels for average channel SNRs below ~20dB. However, as the K factor increased, both the BER and BPS performance was more undulating. This was because the variance of the fading amplitude PDF reduces as the K factor is increased. Consequently, for larger values of K switch from one modulation scheme to another as the average channel SNR increases becomes more dicrete. When using the Rayleigh-optimised switching levels over Rician channels exhibiting K factors of both 4 and 16, the BER never exceeded twice the desired BER, and was often below it in the average channel SNR range from 0 to 20dB. Above average SNRs of 20dB the BER performance over Rician channels improved dramatically, as the K factor was increased. This was the result of a significant reduction in the probability of deep fades.

 28 March 1996
Electronics Letters Online No: 19960799

J.M. Torrance and L. Hanzo (*Department of Electronics and Computer Science, University of Southampton, Southampton SO17 1BJ, United Kingdom*)

References

1 TORRANCE, J. M., and HANZO, L.: 'On the upper bound performance of adaptive modulation in a slow Rayleigh fading channel', *Electron. Lett.*, 1996, **32**, (8), pp. 718–719

2 KAMIO, Y., SAMPEI, S., SASAOKA, H., and MORINAGA, N.: 'Performance of modulation-level-control adaptive-modulation under limited transmission delay time for land mobile communications'. 45th Veh. Technol. Conf., 1995, IEEE, pp. 221–225

3 WEBB, W.T., and HANZO, L.: 'Modern quadrature amplitude modulation' (Pentech Press, 1994)

4 PRESS, W.H., TEUKOLSKY, S. A., VETTERLING, W. T., and FLANNERY, B. P.: 'Numerical recipes in C' (Cambridge University Press, 1994)

Parallel code acquisition technique for preamble search in the CDMA reverse link

Y.H. You, Y.C. Lee, T.H. Moon and C.E. Kang

Indexing terms: Code division multiple access, Spread spectrum communication

A parallel PN code acquisition technique for slotted-mode preamble search in a CDMA reverse link is presented. For received PN codes with different signal-to-noise ratios (SNRs), this scheme provides a sub-optimal threshold value such that the mean acquisition time is minimised.

Introduction: In recent years, some parallel acquisition schemes have been proposed in which a number of cells, less than the number of uncertainty region cells, are tested simultaneously [1 – 3]. Generally, a parallel acquisition system tests all possible code phases and can therefore significantly reduce the mean acquisition time, but at the expense of hardware complexity.

For code acquisition in the code division multiple access (CDMA) reverse link, the mobile transmits a preamble (unmodulated PN sequence) preceding the access slot message, which has been aligned with the pilot signal through the code acquisition in the forward link (base station-to-mobile). At the base station, the code phase of the signal transmitted by the mobile is retarded by round-trip-delay compared with that of the pilot signal. Therefore, the uncertainty region where the code phase of the received signal may be located is quite small in the reverse link, depending on the maximum distance between the base station and the mobile.

In this Letter, a threshold decision technique for the parallel PN code acquisition system is proposed. As a measure of system performance, an expression for the mean acquisition time is derived for the proposed system in terms of the probabilities of detection and false alarm, and its insensitivity to the weighting factor, used to scale the sum ofthe output ofthe reference filter, is highlighted. These parameters are analysed for the nonselective Rayleigh fading channel. The performance of the proposed parallel acquisition system is compared to the conventional parallel acquisition system, and it is shown that a sub-optimal mean acquisition time performance can be achieved thanks to the desired threshold setting for received PN codes with different signal-to-noise ratios (SNRs).

System description: The search mode, as shown in Fig. 1, consists of a bank of N parallel detecting I-Q passive noncoherent PN matched filters and a reference I-Q PN matched filter (PNMF). The I-Q PNMF's structure is the same as that in [4]. The number of taps on each delay line is M/Δ, with ΔT_c delay between successive taps, where M is the MF length, Δ is 2^{-n} for some n = 0, 1, 2, ..., and T_c is the chip duration. The uncertainty region θ of the input code phase is divided into subsequences each with length $M = \theta/N$. In the CDMA forward link, the uncertainty region θ is the full code length L, whereas in the reverse link $\theta \ll L$. Each of the N detecting I-Q PNMF MF_D has, as a reference input, one of the subsequence of length M, and the reference I-Q PNMF MF_R is loaded with a PN code orthogonal to the transmitted PN code [5].

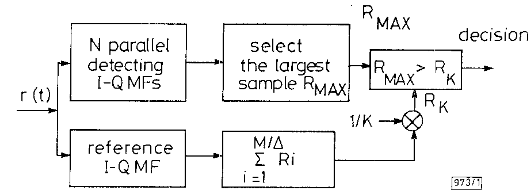

Fig. 1 *Parallel acquisition system*

The initial threshold R_{TH} is set to zero. Every ΔT_c seconds, the proposed system chooses the largest of the resulting N samples. If the largest sample exceeds the threshold value R_{TH}, the corresponding phase is accepted tentatively as the true phase of the received signal. Moreover, R_{TH} is updated to the value of the sample that exceeded the previous threshold. After MT_c seconds, the largest of MN/Δ samples is stored in R_{TH}; at the same time, the sum of M/Δ samples of the reference filter is divided by weighting factor K, where K is an integer which constitutes a fundamental design parameter. If the largest of MN/Δ samples exceeds R_K, which is the sum divided by K, the system is said to have acquired the code phase of the signal. Otherwise, the system waits for the next slot. This method avoids the need for large memory and the problem of recording the delay of each sample stored in the memory. Most code acquisition systems use the verification mode to confirm whether or not the tentative decision is true. However, in the CDMA reverse link, an error handling technique for slotted-mode preamble search, such as a cyclic redundancy check, is used instead of the verification mode [6].

Detection performance acquisition system: In our analysis we consider a nonselective Rayleigh fading channel as in [1], where the fading process is regarded as a constant over k successive chips $k \ll M$, and these successive groups of k chips are correlated. In deriving the probability expressions, we shall adopt the same assumptions used in [3]. Under hypothesis H_i: i = 0, 1, e_I and e_Q follow the zero-mean Gaussian distribution with variances $\sigma_0^2 = MT_c^2\sigma_s^2 + \sigma_n^2$ and $\sigma_1^2 = WT_c^2\sigma_s^2 + \sigma_n^2$, respectively, where W is the conditional variance of a correct cell normalised by in-phase (or quadrature) signal variance as defined in [1]. Thus, the probability density function (PDF) of $R_i = e_I^2 + e_Q^2$ under hypothesis H_0 and H_1, follows the χ^2 distribution with two degrees of freedom. Referring to Fig. 1, R_K that is the threshold value of the search mode is expressed as

$$R_K = \frac{1}{K}\sum_{i=1}^{M/\Delta} R_i \tag{1}$$

For the case of the considered fading channel, it can be readily shown that, assuming that the reference code and the transmitted code in MF_R are purely orthogonal, the variance of the output of each of the MF correlators in MF_R is given by σ_0^2. From this assumption, the PDF of R_K follows the χ^2 distribution with M/ΔD degrees of freedom

$$p_{R_K}(y) = \frac{K^{M/\Delta}}{(2\sigma_0^2)^{M/\Delta}\Gamma(M/\Delta)} y^{M/\Delta-1}\exp\left(-\frac{Ky}{2\sigma_0^2}\right) \tag{2}$$

The detection probability of the search mode P_D is the probability that the H_1 cell is larger than all θ/Δ–1 cells and larger than threshold R_K, which is given by

$$P_D = \sum_{n=0}^{\theta/\Delta-1}(-1)^n\binom{\theta/\Delta-1}{n} \times \left[\frac{1+\gamma_c}{1+\gamma_c+n(1+\gamma_c W/M)} - \frac{1+\gamma_c}{K(1+\gamma_c W/M)} \times \sum_{k=0}^{M/\Delta-1}\left\{\frac{K(1+\gamma_c W/M)}{1+\gamma_c+(n+K)(1+\gamma_c W/M)}\right\}^{k+1}\right] \tag{3}$$